Available online at www.sciencedirect.com
ScienceDirect
Trans. Nonferrous Met. Soc. China 29(2019) 754−763
Transactions of Nonferrous Metals Society of China
www.tnmsc.cn

Brazeability evaluation of Ti−Zr−Cu−Ni−Co−Mo filler for vacuum brazing TiAl-based alloy

Li LI[1,2], Xiao-qiang LI[2], Ke HU[2,3], Bo-lin HE[1], Hua MAN[1]

1. School of Materials Science and Engineering, East China Jiaotong University, Nanchang 330013, China;
2. National Engineering Research Center of Near-net-shape Forming for Metallic Materials, South China University of Technology, Guangzhou 510640, China;
3. National Engineering Research Center of Powder Metallurgy of Titanium & Rare Metals, Guangdong Institute of Materials and Processing, Guangzhou 510650, China

Received 8 June 2018; accepted 19 November 2018

Abstract: Ti−47Al−2Nb−2Cr−0.15B (mole fraction, %) alloy was vacuum brazed with amorphous and crystalline Ti−25Zr−12.5Cu−12.5Ni−3.0Co−2.0Mo (mass fraction, %) filler alloys, and the melting, spreading and gap filling behaviors of the amorphous and crystalline filler alloys as well as the joints brazed with them were investigated in details. Results showed that the amorphous filler alloy possessed narrower melting temperature interval, lower liquidus temperature and melting active energy compared with the crystalline filler alloy, and it also exhibited better brazeability on the surface of the Ti−47Al−2Nb−2Cr−0.15B alloy. The TiAl joints brazed with crystalline and amorphous filler alloys were composed of two interfacial reaction layers and a central brazed layer. Under the same conditions, the tensile strength of the joint brazed with the amorphous filler alloy was always higher than that with the crystalline filler alloy. The maxmium tensile strength of the joint brazed at 1273 K with the amorphous filler alloy reached 254 MPa.
Key words: vacuum brazing; Ti−47Al−2Nb−2Cr−0.15B alloy; amorphous Ti−25Zr−12.5Cu−12.5Ni−3.0Co−2.0Mo filler alloy; tensile strength; interfacial microstructure; brazeability

1 Introduction

TiAl-based alloys are considered as the most promising alternative light-weight heat-resistant materials due to their outstanding properties such as relatively low density, high service temperature of 1033−1123 K, excellent high-temperature strength retention as well as corrosion and oxidation resistance, high specific strength and elastic modulus [1−4]. They have great potential to replace traditional Ni-based superalloys and heat-resistant steels in aerospace and automotive industries for significant weight saving [5−7]. However, the wide applications of TiAl alloys have been restricted due to their intrinsic brittleness and poor workability as well as high cost [8]. In order to widen the applications of TiAl alloys in real components, it is necessary to join TiAl alloys to themselves or to other materials. According to the works reported by SI et al [8] and TETSUI [9], the brazing is considered to be the most feasible and economical technique to join TiAl alloys by comparative discussion about the advantages and disadvantages of fusion welding, friction welding, diffusion bonding and brazing. Moreover, the brittle oxides and intermetallic compounds are easily formed in the brazed joints due to the high reactivity of TiAl alloys, which can cause deterioration of the wettability and the bonding strength. Accordingly, vacuum brazing has been considered as a good choice for joining TiAl alloys.

The selection of filler alloys is important in obtaining robust TiAl brazed joints. Compared with Al-based or Ag-based filler alloys, the TiAl joints brazed with Ti-based filler alloys present better bonding strength and corrosion resistance due to good wettability and

Foundation item: Project (51865012) supported by the National Natural Science Foundation of China; Project (2016005) supported by the Open Foundation of National Engineering Research Center of Near-net-shape Forming for Metallic Materials, China; Project (GJJ170372) supported by the Science Foundation of Educational Department of Jiangxi Province, China; Project (JCKY2016603C003) supported by the GF Basic Research Project, China; Project (JPPT125GH038) supported by the Research Project of Special Furnishment and Part, China
Corresponding author: Xiao-qiang LI; Tel: +86-20-87111080; E-mail: lixq@scut.edu.cn
DOI: 10.1016/S1003-6326(19)64985-X

compatibility between Ti-based filler alloys and TiAl substrates [4,8−10]. According to Refs. [2−4,11], Ti−Zr−Cu−Ni system filler alloy was used to braze TiAl alloys widely. The joint brazed with Ti−Zr−Cu−Ni−Co filler alloy possessed lower hardness and 86.6% higher joint strength than that with Ti−Zr−Cu−Ni filler alloy [2]. QIU et al [3] investigated the effect of Mo additive upon the TiAl brazed joints, and the results revealed that the addition of Mo particles could inhibit the eutectoid transformation of β-Ti and remarkably raised the joint strength. Based on the above results, both Co and Mo are added into Ti−Zr−Cu−Ni filler alloy with the aim to improve the microstructure of the TiAl brazed joint and to enhance the bonding properties.

The wetting, spreading and filling behaviors of filler alloys are inevitably involved during brazing. Hence, the evaluation of brazeability (such as wettability, spreadability and clearance fillability) of the liquid filler alloy on the parent-metal is vitally important, which is also beneficial to determining the brazing parameters. Wettability and spreadability tests are generally performed by the sessile drop method. However, the wetting and spreading behaviors characterized by using the sessile drop method are not satisfactory in the actual brazing process. The experimental parameters and conditions for the wettability and spreadability tests are thus identical to those selected during the brazing process in this study. Researches of gap filling ability have gained great attention and have been conducted by many researchers, but the study on the clearance fillability of liquid Ti-based filler alloy over the TiAl alloys has been scarcely reported.

In this work, the thermal analyses of the amorphous and crystalline Ti−Zr−Cu−Ni−Co−Mo filler alloys and their spreading and gap filling behaviors on Ti−47Al−2Nb−2Cr−0.15B (mole fraction, %) alloy were studied, and the brazing was then performed in vacuum furnace in the temperature range of 1198−1323 K for 10 min. In particular, the effects of brazing temperature on the interfacial microstructure and mechanical properties of the TiAl brazed joints were investigated.

2 Experimental

In this study, γ-TiAl alloy (Ti−47Al−2Nb−2Cr−0.15B (mole fraction, %)) used as parent-metal was firstly fabricated by induction skull melting under high-vacuum atmosphere and then treated at 1173 K for 40 h and hot isostatically-pressed at 1533 K and 135 MPa for 4 h under high purity argon atmosphere. The Ti−25Zr−12.5Cu−12.5Ni−3.0Co−2.0Mo (mass fraction, %) alloy buttons were prepared by arc-remelting in a water-cooled copper crucible under high purity argon atmosphere. Alloy buttons were turned and remelted at least six times for homogenization. A diffusion-annealing treatment was conducted at 1000 K for 8 h to reduce the segregation of the alloy buttons. The prepared alloy buttons were used as crystalline filler and broken into small particles. The particles were produced into alloy ribbons by single roller melt-spinning technique. The resulting ribbon exhibited a thickness of 30−40 μm and a width of about 10 mm. The amorphous nature of the ribbon was identified by the XRD pattern, as shown in Fig. 1. The melting behaviors of the filler alloys (both crystalline and amorphous states) were measured by differential scanning calorimetry (DSC) at heating rates of 0.167—0.667 K/s.

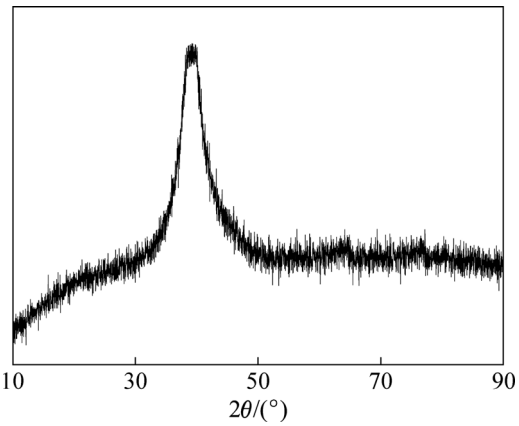

Fig. 1 XRD pattern of melt-spinning Ti−25Zr−12.5Cu−12.5Ni−3.0Co−2.0Mo (mass fraction, %) ribbon

The sizes of the γ-TiAl samples for brazing, spreadability test and clearance fillability test were (12 mm × 3 mm) × 48 mm, (24 mm × 24 mm) × 3 mm and (100 mm × 1 mm) × 12 mm, respectively. All of the stand-by surfaces were polished by SiC papers up to grit 1000 and ultrasonically cleaned by acetone for 10 min. For both crystalline filler and amorphous filler, about 20 μm thick foils were used for brazing and the consumptions for spreadability or clearance fillability tests were 0.5 g. The filler alloys were also cleaned ultrasonically in acetone for 600 s. Prior to brazing, assessments of spreadability and clearance fillability (the corresponding filling clearance was also about 20 μm) of both filler alloys on TiAl alloy were performed according to the National Standard of China (GB/T 11364−2008) in an HP−12×12×12 vacuum furnace with a vacuum of ~1.33×10^{-2} Pa to determine the brazing parameters. The furnace was heated to the experimental temperature (1198−1323 K) at a rate of 0.333 K/s and the holding time was varied from 0 to 20 min, followed by a furnace cooling to room temperature. Subsequently, the monolayer filler foil was sandwiched between two γ-TiAl samples and then the assembled butt joint samples were brazed in an HP−12×12×12 vacuum furnace. Brazing temperatures employed were 1198−1323 K and

the brazing time was 10 min.

The γ-TiAl brazed joints were cut into tensile samples and metallographic specimens according to the schematic diagram, as shown in Fig. 2. A scanning electron microscope (SEM) equipped with an energy dispersive spectrometer (EDS) was used to characterize the microstructures and analyze chemical composition of the brazed joints. Tensile tests were conducted at a constant speed of 1.67×10^{-6} m/s by a universal testing machine. The spreading areas were calculated by means of AutoCAD software and the lengths of gap-filling were measured by a steel rule. Each set of experimental data was determined by at least five tests under the identical conditions.

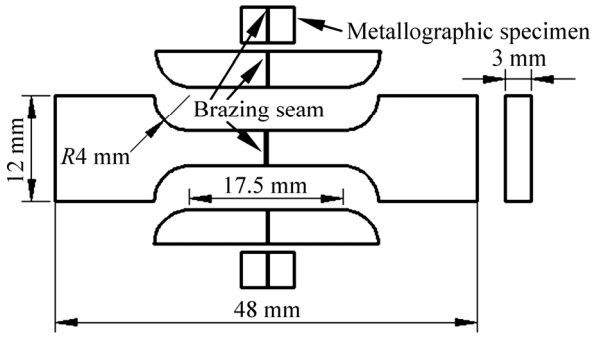

Fig. 2 Schematic diagram of tensile sample and metallographic specimens

3 Result and discussion

3.1 Thermal analyses of filler alloys

Figure 3 shows the DSC curves of crystalline and amorphous Ti−Zr−Cu−Ni−Co−Mo filler alloys at different heating rates. For both filler alloys, the melting peak's height and melting range increase with the increase of heating rate. The melting range between liquidus temperature and solidus temperature of the amorphous filler is obviously narrower than that of the original crystalline filler under same heating rate, which is beneficial to reducing void/crack formation in the brazed joint and to improve the quality of the brazed joint. The differences in melting range may be attributed to different morphologies, i.e., the amorphous filler alloy after crystallization exhibits a more even and finer microstructure compared with the original crystalline filler alloy. Table 1 summarizes the characteristic temperatures for the Ti−Zr−Cu−Ni−Co−Mo filler alloy at different heating rates. The solidus temperatures (T_s), melting peak temperatures (T_p) and liquidus temperatures (T_l) of the crystalline and amorphous filler alloys increase with the increase of heating rate, indicating that the melting behavior is significantly dependent on the heating rate. Moreover, at the same heating rate, both T_l and T_p for the amorphous filler alloy are lower than those for the crystalline filler alloy, but a reverse result is obtained for T_s. At a heating rate of 0.333 K/s, T_l and T_s for the amorphous filler alloy in this study are 25.8 K lower and 8 K higher than those in our previous research [12], respectively. The same phenomenon is also found in the crystalline filer. This indicates that the composition of the developed filler alloy in this study is closer to the eutectic point.

Combining DSC results and limiting heating rate of the vacuum furnace used in this study, 1184.0 and 1147.2 K obtained at a heating rate of 0.333 K/s were selected as the liquidus temperatures (T_l) of the crystalline and amorphous filler alloys, respectively. In general, the brazing temperature should be at least 10 K above the liquidus temperature to ensure that the filler

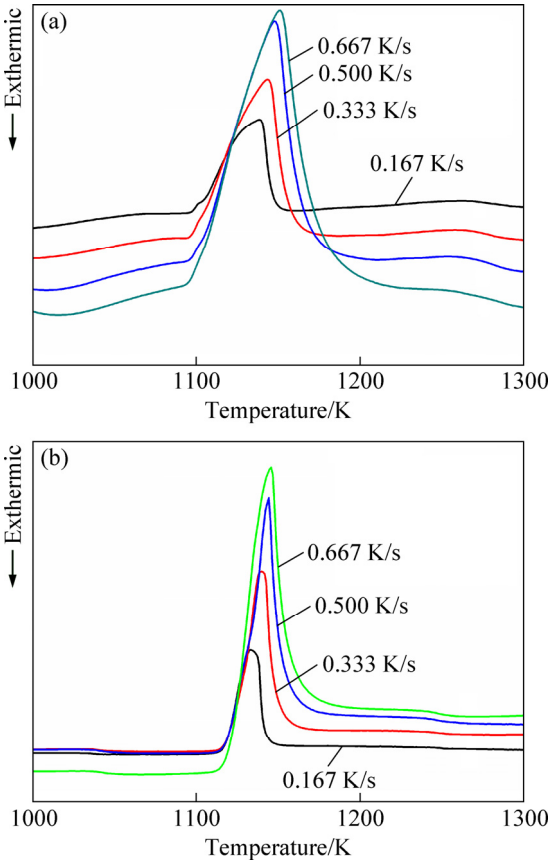

Fig. 3 DSC curves of Ti−Zr−Cu−Ni−Co−Mo filler alloys at different heating rates: (a) Crystalline; (b) Amorphous

Table 1 Characteristic temperatures T_s, T_p and T_l of Ti−Zr−Cu−Ni−Co−Mo filler at different heating rates

Heating rate/ (K·s^{-1})	Crystalline filler			Amorphous filler		
	T_s/K	T_p/K	T_l/K	T_s/K	T_p/K	T_l/K
0.167	1092.0	1138.8	1161.0	1118.0	1132.9	1140.7
0.333	1093.0	1143.8	1184.0	1124.0	1140.1	1147.2
0.500	1094.0	1148.3	1205.0	1129.0	1144.0	1173.0
0.667	1095.0	1150.9	1228.0	1132.0	1145.7	1180.0

alloy is entirely melted during brazing [13]. Furthermore, SONG et al [14] pointed out that the solid-state phase transformation and disordered transformation would occur in TiAl alloy when the temperature was above 1373 K. Therefore, the brazing temperatures ranging from 1198 to 1323 K were selected in this study.

At present, the Kissinger method is used to determine the kinetic constant of phase transformation observed using DSC [15−17]. The activation energy (E, reflecting the barrier energy needed to be overcome) can be calculated by the Kissinger equation [18,19]:

$$\ln\left(\frac{T^2}{\beta}\right)=-\frac{E}{RT}+\text{const.} \quad (1)$$

where T is the characteristic temperature corresponding to the heating rate β; R is the mole gas constant. In a certain sense, the melting process of alloy can be considered as phase transformation. Therefore, the melting activation energy of the filler alloy can be calculated via Kissinger equation. For both filler alloys, E can be obtained by plotting $\ln(T^2/\beta)$ versus $1000/(RT)$, as shown in Fig. 4. E_s, E_p and E_l of the crystalline filler alloy, corresponding to T_s, T_p and T_l, are 4520.1, 1207.8 and 224.7 kJ/mol, respectively. Significantly, E_s is much higher than E_p and E_l. This means that relatively high barrier energy must be overcome at the initial melting stage. For the amorphous filler alloy, the E_s, E_p and E_l are 1010.0, 1116.4 and 309.4 kJ/mol, respectively. The difference between E_s and E_p is small, but they are much higher than E_l. Compared with the crystalline filler alloy, the E_s and E_p of amorphous filler alloy are lower, but E_l is slightly higher. Accordingly, the amorphous filler alloy overcomes lower barrier energy during melting, in contrast to the crystalline filler alloy. Thus, we believe that the amorphous filler alloy has a better melting characteristic compared with the crystalline filler alloy, which can improve the wettability, spreadability and clearance fillability of molten filler alloy as well as bonding quality of brazed joints.

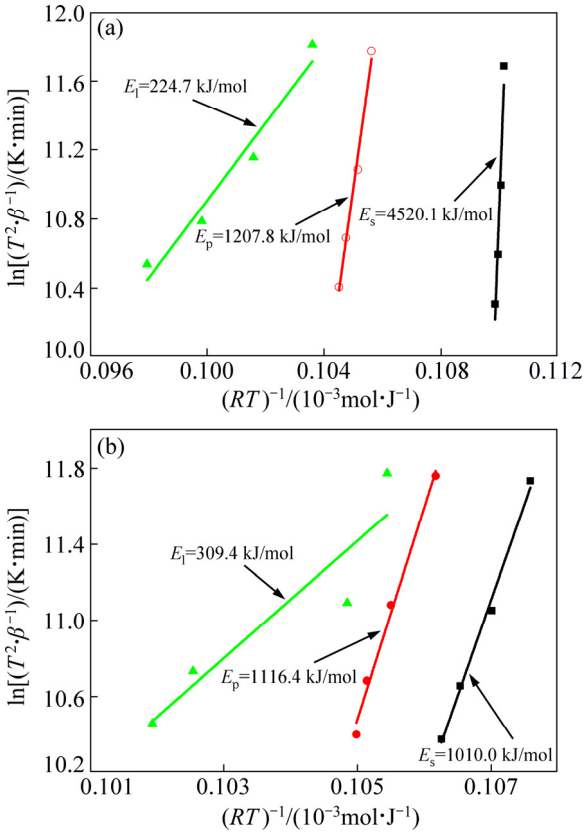

Fig. 4 Kissinger plots of Ti−Zr−Cu−Ni−Co−Mo filler alloys: (a) Crystalline; (b) Amorphous

3.2 Brazeability of filler alloys

Figure 5(a) shows the effect of testing temperature on the spreading areas of the crystalline and amorphous Ti−Zr−Cu−Ni−Co−Mo filler alloys at testing time of 10 min. Results show that the spreading area increases with the increase of testing temperature. This indicates that the atomic diffusion and metallurgical bonding between the TiAl alloy and the filler alloy are enhanced with the increase of testing temperature, which can improve the wettability and spreadability of the molten filler alloy on TiAl alloy. It is noted that the increment of spreading area firstly increases and then decreases and the boundary ridge of testing temperature is around 1248 K. The same phenomena were also found elsewhere [20,21]. When the testing temperature is 1248 K, the effect of testing time on the spreading areas of crystalline and amorphous Ti−Zr−Cu−Ni−Co−Mo filler alloys is shown in Fig. 5(b). Significantly, the increase of testing time leads to an increase in the spreading area and a trend of stalemate after 10 min. The final equilibrium spreading areas for the crystalline and amorphous filler alloys at 1248 K are about 228 and 286 mm^2, respectively. It is worthy to note that the spreading area of the amorphous filler alloy is obviously larger than that of the crystalline filler alloy under the same conditions, suggesting that the molten amorphous filler has a better wettability or spreadability on the TiAl alloy. It may be caused by the narrower melting temperature interval between liquidus temperature and solidus temperature, and lower liquidus temperature for the amorphous filler alloy. And it may also well be included the lower E_s and E_p, unique supercooled liquid region during melting. YANG et al [22] reported that the larger melting range between liquidus temperature and solidus temperature could increase the viscosity and lower the fluidity of filler alloys, thereby decreasing the wettability. KIM and LEE [23] stated that the wettability of molten filler alloy on the same substrate decreased with their increasing melting temperature for the same chemical composition filler alloy. Their results

further prove that our inference is correct. Finally, the holding time of clearance fillability test and brazing is identified as 10 min on account of the above results of wettability and spreadability tests.

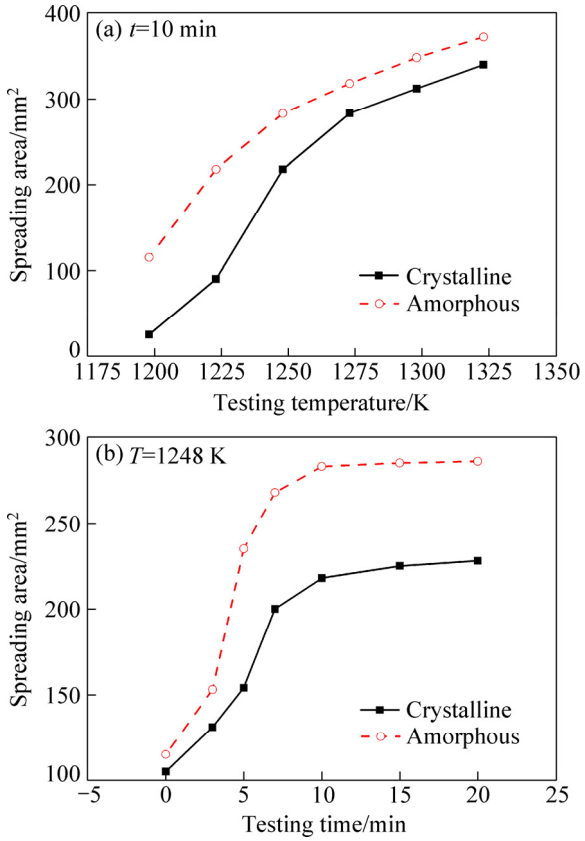

Fig. 5 Effects of testing temperature (a) and testing time (b) on spreading areas of crystalline and amorphous Ti−Zr−Cu−Ni−Co−Mo filler alloys

Figure 6 shows the macrographs of the samples after clearance fillability testing at different temperatures for 10 min. The length of gap filling reaches 100 mm at the temperature of 1248 K for the amorphous filler alloy but at 1298 K for the crystalline filler alloy. At the same testing temperature, much higher and wider brazing toe in the seam filled with the amorphous filler alloy demonstrates that the amorphous filler alloy exhibits better fillability and adhesiveness compared with the crystalline filler alloy. In a word, the amorphous filler alloy possesses better brazeability (wettability and spreadability, fillability and adhesiveness) than the crystalline filler alloy.

3.3 Interfacial microstructure of brazed joints

Figure 7 shows the backscattered electron image of the TiAl joint brazed with the amorphous filler alloy at 1198 K for 10 min. It can be seen that a sound TiAl brazed joint is obtained without any imperfections such as voids and cracks. Moreover, the width of the brazing seam is about 25 μm, which is wider than the original

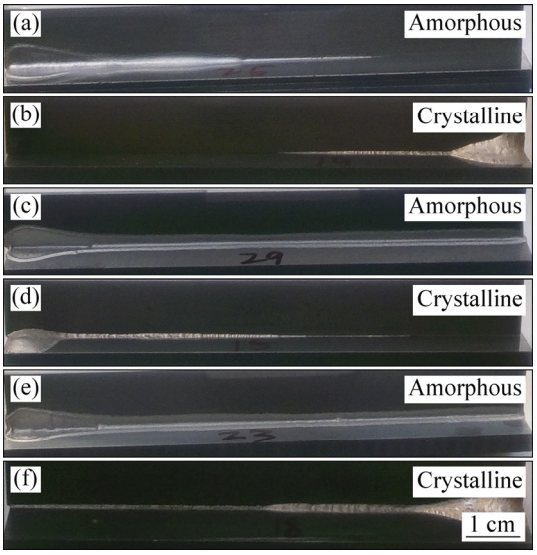

Fig. 6 Macroscopic photos of clearance fillability test samples at 1198 K (a, b), 1248 K (c, d), and 1298 K (e, f) for 10 min

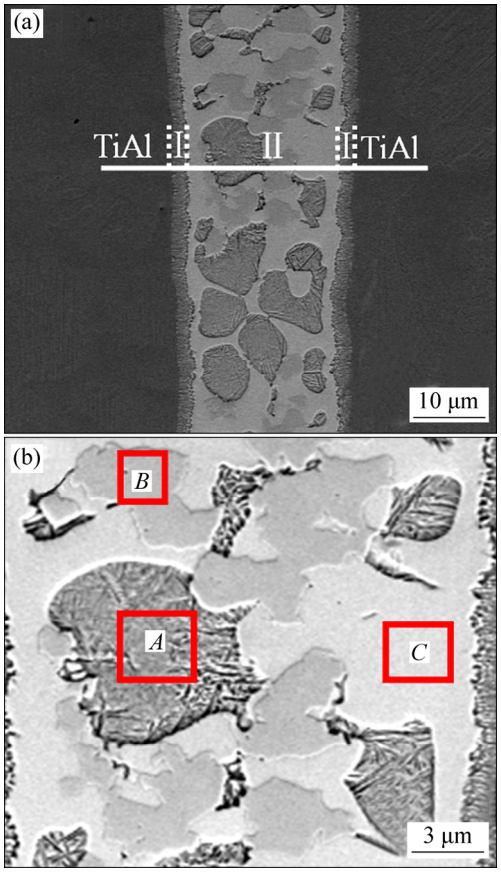

Fig. 7 Backscattered electron images of TiAl joint brazed with amorphous filler alloy at 1198 K for 10 min: (a) Whole joint; (b) Magnification of layer II

joint clearance (~20 μm). This indicates that intensive interaction between TiAl alloy and the molten filler alloy occurs during brazing. Based on the microstructural morphology and the chemical composition, the brazing

seam mainly consists of a central brazed layer II between two interfacial reaction layers I. According to the difference in contrast, it can be inferred that the central layer II was a three-phase mixed region (marked as *A*, *B* and *C*). Generally, in the backscattered electron image, the dark phase has lower atomic number in comparision with the bright matrix [24]. Therefore, it can be inferred that Area *A* has the lowest atomic number and the maximum atomic number is in Area *C*, which is further confirmed by the EDS results in Table 2. According to Ti−Al binary phase diagram (see Refs. [4,8]) and the EDS results of Zone I (listed in Table 2), we deduce that Zone I mainly consists of α_2-Ti_3Al phase and the phases in the central layer II can be identified as α-(Ti,Zr) with γ-$(Ti,Zr)_2(Cu,Ni)$ (Spot *A*), γ-$(Ti,Zr)_2(Cu,Ni)$ with α-(Ti,Zr) (Spot *B*) and γ-$(Ti,Zr)_2(Cu,Ni)$ (Spot *C*). It is noted that the α-(Ti,Zr) is beneficial to the strength of the brazed joint but the γ-$(Ti,Zr)_2(Cu,Ni)$ is the opposite.

Figure 8 shows the backscattered electron images of the TiAl joints brazed with crystalline and amorphous filler alloys under the brazing temperatures ranging from 1223 to 1298 K for 10 min. It can be seen that all the brazed joints mainly consist of a central brazed layer II between two interfacial reaction layers I regardless of the brazing temperature and the state of filler alloy. The degree of TiAl alloy dissolution into the molten filler alloy is greatly dependent on the brazing temperature, which is the major controlling factor to the interfacial microstructure of the TiAl brazed joint [3]. The interfacial morphology of the brazing seam, especially the interfacial reaction layer I and Ti−Zr-rich phase (marked as *A* in Fig. 7) in the central brazed layer II, changes significantly with the brazing temperature. The joints brazed with the crystalline filler are free of defects when the brazing temperature is below 1248 K; and then an increase of micro-voids occurs in the central brazed layer II when the temperature is above 1248 K. The unexpected micro-voids may be resulted from the wider melting temperature interval and the variation of brazing toe when the temperature exceeds 1248 K (as shown in Fig. 6). High quality TiAl joints devoid of imperfections, brazed with the amorphous filler alloy, are obtained at temperatures ranging from 1223 to 1273 K and micro-cracks occur with further increase of the brazing temperature. The micro-voids and micro-cracks are detrimental and they should be avoided to obtain a robust joint. In addition, the thickness of the interfacial reaction layer I of the TiAl joint brazed with amorphous filler increases with the increase of brazing temperature, which is always wider than that brazed with the crystalline filler alloy at the same temperature. This demonstrates that the interaction between TiAl alloy and the amorphous filler alloy and the dissolution of TiAl alloy into the molten origin amorphous filler are stronger, in contrast to the crystalline filler alloy. This superiority is attributed to the narrower melting temperature interval and better brazeability of the amorphous filler alloy (the afore-mentioned results of the thermal analysis as well as spreadability test and clearance fillability test).

3.4 Tensile strength of brazed joints

Figure 9 shows the variation of average room temperature (RT) tensile strength of the TiAl joints respectively brazed with crystalline and amorphous filler alloys at different brazing temperatures for 10 min. It is obvious that the tensile strength of the brazed TiAl joints firstly increases and then decreases with the increase of brazing temperature. When the brazing temperature is 1198 K, the tensile strength of the joint brazed with crystalline filler alloy is only 63 MPa, much less than that brazed with the amorphous filler alloy (188 MPa). The main cause for the difference is the different temperature intervals between the brazing temperature and the liquidus temperature of the filler alloys, e.g., the interval is 14 K for the crystalline filler alloy, but it is up to 50.8 K for the amorphous filler alloy. In general, a large temperature interval between the brazing temperature and the liquidus temperature of the filler alloy can improve the atomic diffusion and dissolution reaction between the molten filler alloy and the parent metal, leading to an enhanced metallurgical reaction and chemical joining [25−29]. Actually, increasing the brazing temperature is equal to increasing the temperature interval between the brazing temperature and the liquidus temperature of the filler alloy. Therefore,

Table 2 EDS results of each spot and zones I and II in Fig. 7

Zone	Mole fraction/%									Possible phase
	Ti	Zr	Cu	Ni	Al	Co	Mo	Nb	Cr	
A	71.0	5.5	8.0	5.1	6.1	2.4	1.7	0.1	0.1	α-(Ti,Zr) with γ-$(Ti,Zr)_2(Cu,Ni)$
B	58.4	9.0	7.6	17.7	2.0	2.7	1.8	0.2	0.6	γ-$(Ti,Zr)_2(Cu,Ni)$ with α-(Ti,Zr)
C	34.6	20.6	15.3	14.8	10.9	1.6	1.6	0.4	0.2	γ-$(Ti,Zr)_2(Cu,Ni)$
I	62.8	5.0	4.3	2.6	22.2	0.8	0.7	0.9	0.7	α_2-Ti_3Al
II	57.6	10.9	9.6	9.3	8.0	2.3	1.7	0.2	0.4	Including phases in Zones *A*, *B* and *C*

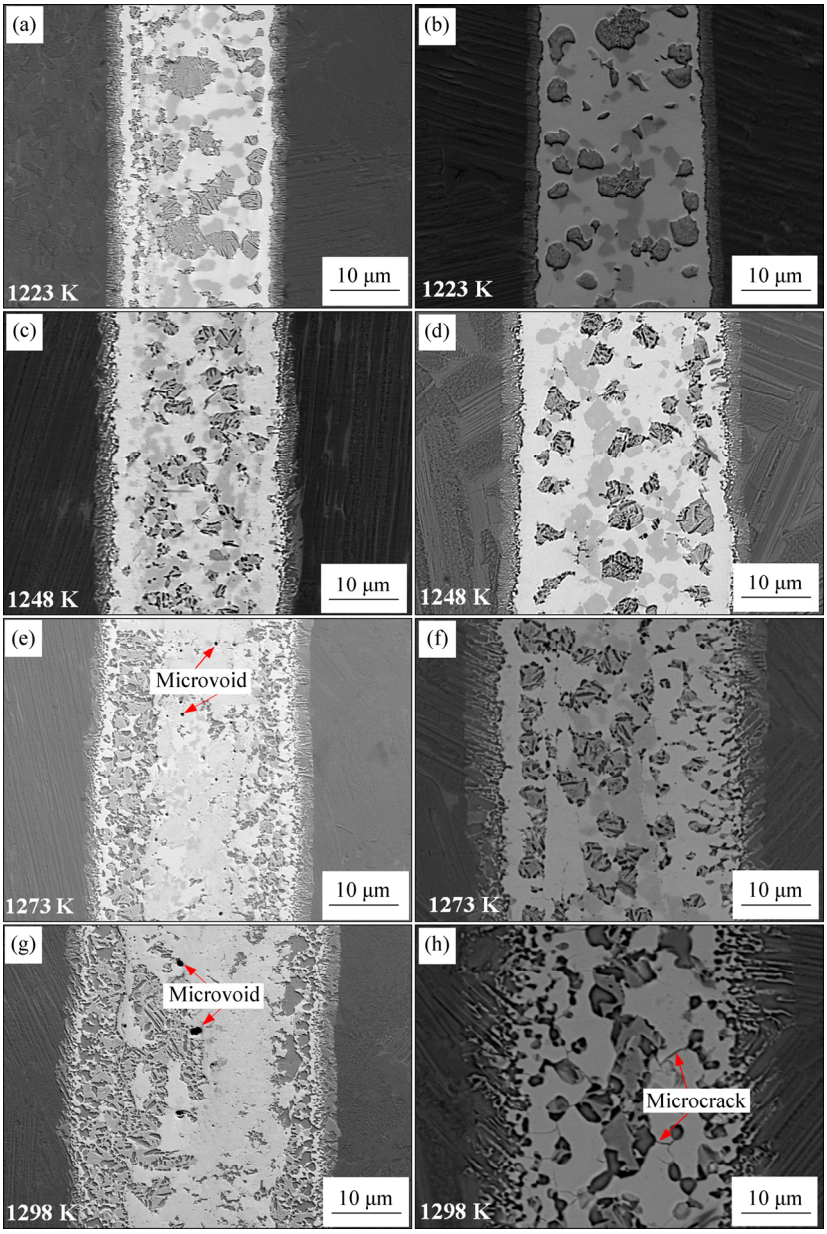

Fig. 8 Backscattered electron images of TiAl joint brazed at different brazing temperatures for 10 min with crystalline filler (a, c, e, g) and amorphous filler (b, d, f, h)

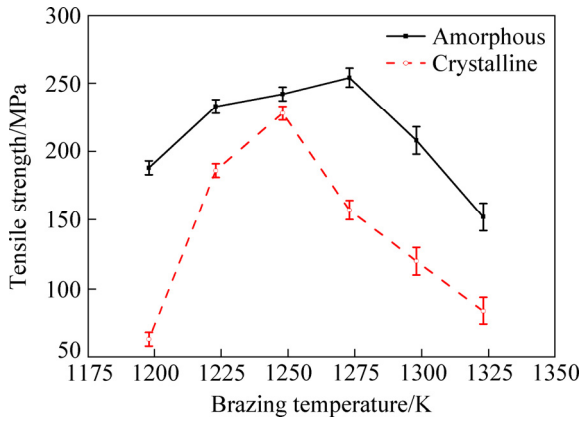

Fig. 9 Effect of brazing temperarure on RT tensile strength of TiAl brazed joints

the tensile strength of the TiAl brazed joint increases with the increase of brazing temperature. The maxmium tensile strength of the TiAl joint is 254 MPa at a brazing temperature of 1273 K for the amorphous filler alloy and 228 MPa at 1248 K for the crystalline filler alloy. However, further increasing the brazing temperature will lead to the formation of micro-voids and micro-cracks as well as an increasing amount of intermetallics in the brazing seams, which act as the sources for stress concentration and the initiation sites of cracks. Therefore, the tensile strength of the TiAl brazed joint turns to decrease with further increasing the brazing temperature. When the brazing temperature increases to 1323 K, the tensile stength decreases to 152 MPa for the joint brazed

with the amorphous filler alloy and 84 MPa for that brazed with the crystalline filler alloy. Moreover, it is important that the tensile strength of the joints brazed with the amorphous filler alloy is always superior to that brazed with the crystaline filler alloy under the same conditions, further showing that the amorphous filler has a better brazeability than the crystalline filler.

Figure 10 shows the typical fracture paths and fracture morphologies of the TiAl joints brazed at different brazing temperatures for 10 min. It can be observed that the cracks primarily propagate along the central brazed layer II and the fracture surface is of a

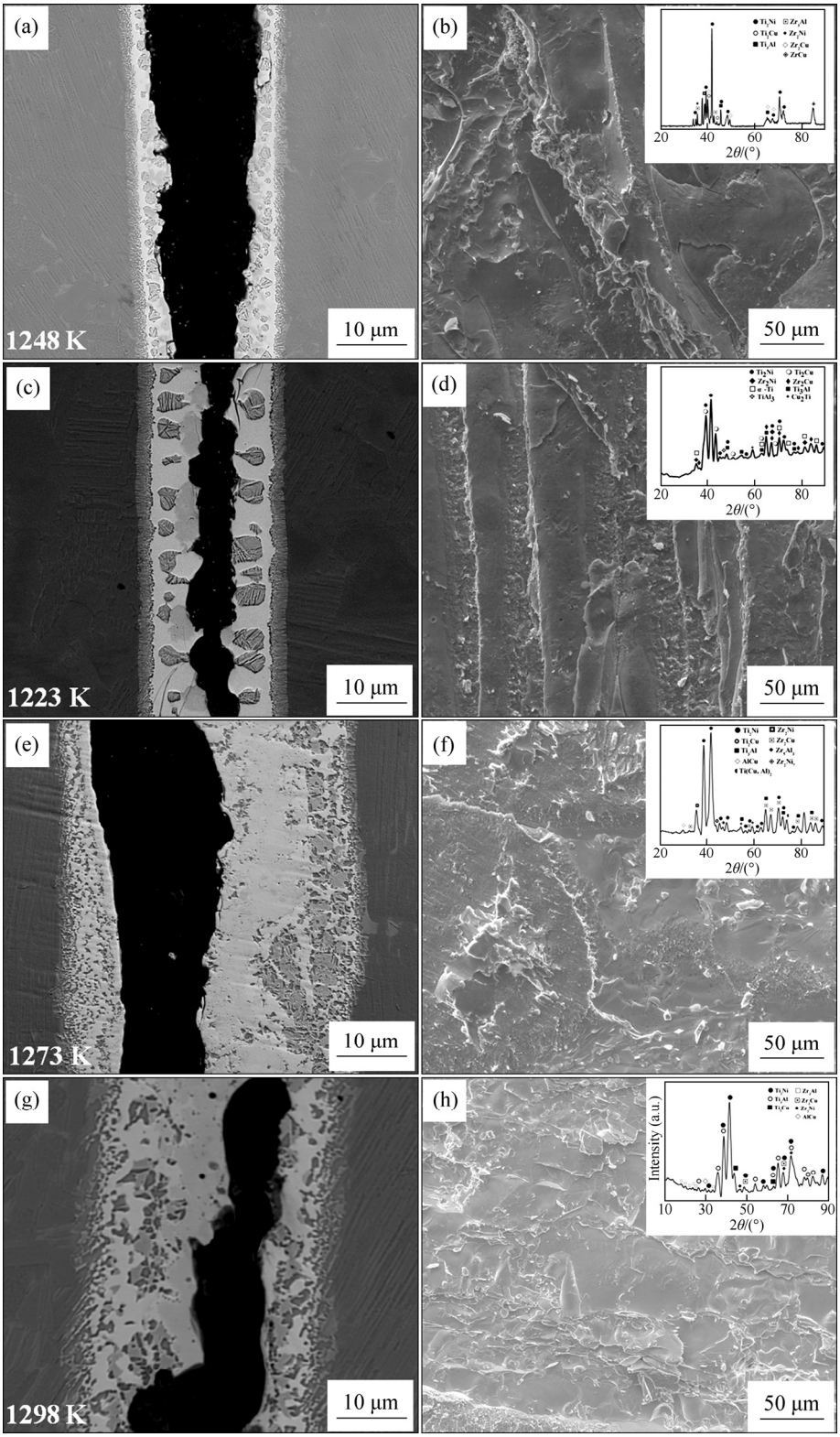

Fig. 10 Typical fracture paths and fracture morphologies of TiAl joints brazed with crystalline filler alloy (a, b, e, f) and amorphous filler alloy (c, d, g, h)

typical cleavage fracture. The XRD analyses of the fracture surfaces (as shown in Figs. 10(b, d, f, h)) indicate that γ-$(Ti,Zr)_2(Cu,Ni)$ intermetallic compounds occupy most of the fracture surfaces. Therefore, the continuous γ-$(Ti,Zr)_2(Cu,Ni)$ intermetallic should be avoided in the brazing seam so as to obtain robust joint.

4 Conclusions

(1) The results of thermal analysis (DSC and apparent activation energy calculation), spreadability and clearance fillability tests reveal that the amorphous filler alloy exhibited better brazeability (wettability and spreadability, fillability and adhesiveness) compared with the crystalline filler alloy, due to its narrower melting temperature interval between solidus temperature and liquidus temperature, lower liquidus temperature and melting active energy, and unique supercooled liquid region during melting.

(2) Compared with the crystalline filler alloy, the TiAl joint brazed with the amorphous filler alloy displayed better tensile strength under the same conditions due to its better brazeability. The maximum average tensile strength of the TiAl joint brazed with the amorphous filler alloy reached 254 MPa when brazing was conducted at 1273 K for 10 min. All the cracks primarily propagated along the central brazed layer II and the γ-$(Ti,Zr)_2(Cu,Ni)$ intermetallic compounds occupied most of the fracture surfaces.

References

[1] XU Wen-chen, HUANG Kai, WU Shi-feng, ZONG Ying-ying, SHAN De-bin. Influence of Mo content on microstructure and mechanical properties of beta-containing TiAl alloy [J]. Transactions of Nonferrous Metals Society of China, 2017, 27(4): 820−828.

[2] REN H S, XIONG H P, CHEN B, PANG S J, CHEN B Q, YE L. Vacuum brazing of Ti_3Al-based alloy to TiAl using TiZrCuNi(Co) fillers [J]. Journal of Materials Processing Technology, 2015, 224: 26−32.

[3] QIU Qi-wen, WANG Ying, YANG Zhen-wen, HU Xin, WANG Dong-po. Microstructure and mechanical properties of TiAl alloy joints vacuum brazed with Ti−Zr−Ni−Cu brazing powder without and with Mo additive [J]. Materials and Design, 2016, 90: 650−659.

[4] LI Li, LI Xiao-qiang, HU Ke, QU Sheng-guan, YANG Chao, LI Zhi-feng. Effects of brazing temperature and testing temperature on the microstructure and shear strength of γ-TiAl joints [J]. Materials Science and Engineering A, 2015, 634: 91−98.

[5] XIAO Shu-long, XU Li-juan, CHEN Yu-yong, YU Hong-bao. Microstructure and mechanical properties of TiAl-based alloy prepared by double mechanical milling and spark plasma sintering [J]. Transactions of Nonferrous Metals Society of China, 2012, 22(5): 1086−1091.

[6] SONG X G, CAO J, LIU Y Z, FENG J C. Brazing high Nb containing TiAl alloy using TiNi−Nb eutectic braze alloy [J]. Intermetallics, 2012, 22: 136−141.

[7] FAN Jiang-lei, LI Xin-zhong, SU Yan-qing, CHEN Rui-run, GUO Jing-jie, FU Heng-zhi. Effect of thermal stabilization on microstructure and mechanical property of directionally solidified Ti−46Al−0.5W−0.5Si alloy [J]. Transactions of Nonferrous Metals Society of China, 2012, 22: 1073−1080.

[8] SI X Q, ZHAO H Y, CAO J, SONG X G, TANG D Y, FENG J C. Brazing high Nb containing TiAl alloy using Ti−28Ni eutectic brazing alloy: Interfacial microstructure and joining properties [J]. Materials Science and Engineering A, 2015, 636: 522−528.

[9] TETSUI T. Effect of brazing filler on properties of brazed joints between TiAl and metallic materials [J]. Intermetallics, 2001, 9: 253−260.

[10] NODA T, SHIMIZU T, OKABE M, IIKUBO T. Joining of TiAl and steels by induction brazing [J]. Materials Science and Engineering A, 1997, 239−240: 613−618.

[11] REN H S, XIONG H P, CHEN B, PANG S J, CHEN B Q, YE L. Microstructures and mechanical properties of vacuum brazed Ti_3Al/TiAl joints using two Ti-based filler metals [J]. Journal of Materials Science and Technology, 2016, 32: 372−380.

[12] LI Li, LI Xiao-qiang, LI Zhi-feng, HU Ke, QU Sheng-guan, YANG Chao. Comparison of TiAl-based intermetallics joints brazed with amorphous and crystalline Ti−Zr−Cu−Ni−Co−Mo fillers [J]. Advanced Engineering Materials, 2016, 18(2): 341−347.

[13] DONG Hong-gang, YANG Zhong-lin, YANG Guo-shun, DONG Chuang. Vacuum brazing of TiAl alloy to 40Cr steel with $Ti_{60}Ni_{22}Cu_{10}Zr_8$ alloy foil as filler metal [J]. Materials Science and Engineering A, 2013, 561: 252−258.

[14] SONG X G, CAO J, CHEN H Y, WANG Y F, FENG J C. Brazing TiAl intermetallics using TiNi−V eutectic brazing alloy [J]. Materials Science and Engineering A, 2012, 551: 133−139.

[15] LOUZGUINE D V, INOUE A. Evaluation of the thermal stability of a $Cu_{60}Hf_{25}Ti_{15}$ metallic glass [J]. Applied Physics Letters, 2002, 81(14): 2561−2562.

[16] SHA W. Determination of activation energy of phase transformation and recrystallization using a modified Kissinger method [J]. Metallurgical and Materials Transactions A, 2001, 32(11): 2903−2904.

[17] YAN Z J, HE S R, LI J R, ZHOU Y H. On the crystallization kinetics of $Zr_{60}Al_{15}Ni_{25}$ amorphous alloy [J]. Journal of Alloys and Compounds, 2004, 368: 175−179.

[18] XU Chen-chen, XIAO Xue-zhang, SHAO Jie, LIU Lang-xia, QIN Teng, CHEN Li-xin. Effects of Ti-based additives on Mg_2FeH_6 dehydrogenation properties [J]. Transactions of Nonferrous Metals Society of China, 2016, 26(3): 791−798.

[19] YANG Y J, XING D W, SHEN J, SUN J F, WEI S D, HE H J, MCCARTNEY D G. Crystallization kinetics of a bulk amorphous Cu−Ti−Zr−Ni alloy investigated by differential scanning calorimetry [J]. Journal of Alloys and Compounds, 2006, 415: 106−110.

[20] OSÓRIO W R, GARCIA A. Interrelation of wettability−microstructure−tensile strength of lead-free Sn−Ag and Sn−Bi solder alloys [J]. Science and Technology of Welding and Joining, 2016, 21(6): 429−437.

[21] ZHANG B, LI H, ZHU Z W, FU H M, WANG A M, DONG C, ZHANG H F, HU Z Q. Reaction induced anomalous temperature dependence of equilibrium contact angle of TiZr based glass forming melt on Al_2O_3 substrate [J]. Materials Science and Technology, 2013, 29(3): 332−336.

[22] YANG Jin-long, XUE Song-bai, WU Yang-yang, YU Cheng-Nien, SEKULIC D P. Wetting behaviour of Zn−Al filler metal on a stainless steel substrate [J]. Science and Technology of Welding and Joining, 2018, 23(1): 1−6.

[23] KIM J H, LEE T Y. Brazing method to join a novel $Cu_{54}Ni_6Zr_{22}Ti_{18}$ bulk metallic glass to carbon steel [J]. Science and Technology of Welding and Joining, 2017, 22(8): 714−718.

[24] MIAB R J, HADIAN A M. Effect of brazing time on microstructure and mechanical properties of cubic boron nitride/steel joints [J]. Ceramics International, 2014, 40: 8519−8524.
[25] HE P, FENG J C, XU W. Mechanical property of induction brazing TiAl-based intermetallics to steel 35CrMo using AgCuTi filler metal [J]. Materials Science and Engineering A, 2006, 418: 45−52.
[26] HE P, FENG J C, ZHOU H. Microstructure and strength of brazed joints of Ti_3Al-base alloy with TiZrNiCu filler metal [J]. Materials Science and Engineering A, 2005, 392: 81−86.
[27] HONG I T, KOO C H. Microstructural evolution and shear strength of brazing C103 and Ti−6Al−4V using Ti−20Cu−20Ni−20Zr (wt.%) filler metal [J]. International Journal of Refractory Metals & Hard Materials, 2006, 24: 247−252.
[28] LEE J G, LEE M K. Microstructural and mechanical characteristics of zirconium alloy joints brazed by a Zr−Cu−Al-based glassy alloy [J]. Materials and Design, 2015, 65: 265−271.
[29] ZHANG X P, SHI Y W. A dissolution model of base metal in liquid brazing filler metal during high temperature brazing [J]. Scripta Materialia, 2004, 50:1003−1006.

真空钎焊 TiAl 基合金用 Ti−Zr−Cu−Ni−Co−Mo 钎料的钎焊性能

李 力[1,2]，李小强[2]，胡 可[2,3]，何柏林[1]，满 华[1]

1. 华东交通大学 材料科学与工程学院，南昌 330013；
2. 华南理工大学 国家金属材料近净成形工程技术研究中心，广州 510640；
3. 广东省材料与加工研究所 国家钛及稀有金属粉末冶金工程技术研究中心，广州 510650

摘 要：采用非晶和晶态 Ti−25Zr−12.5Cu−12.5Ni−3.0Co−2.0Mo(质量分数，%)钎料对 Ti−47Al−2Nb−2Cr−0.15B(摩尔分数，%)合金进行真空钎焊连接，对两种钎料的熔化行为、润湿铺展性、填缝隙能力以及由钎焊 TiAl 基合金所得的钎焊接头进行详细的研究。结果表明：与晶态钎料相比，非晶钎料具有更窄的熔化温度区间、更低的液相线温度和熔化激活能；同时，非晶钎料在 Ti−47Al−2Nb−2Cr−0.15B 合金表面上具有更优异的钎焊性。非晶和晶态两种钎料的钎焊接头均由两侧的界面反应层和中心钎焊层组成，非晶钎料钎焊接头的抗拉强度均高于相同钎焊工艺参数下的晶态钎料钎焊接头的抗拉强度，且在钎焊温度 1273 K 下获得的钎焊接头的抗拉强度达到最大值 254 MPa。

关键词：真空钎焊；Ti−47Al−2Nb−2Cr−0.15B 合金；非晶 Ti−25Zr−12.5Cu−12.5Ni−3.0Co−2.0Mo 钎料合金；抗拉强度；界面组织；钎焊性

(Edited by Wei-ping CHEN)